

CHAPTER 5

Computational study on redox reaction of puupehenone in aqueous solution by density functional theory

5.1. Introduction

Lipoxygenases are non-heme iron containing oxidative enzymes, occurring in a number of plants and animals [1, 2]. These enzymes catalyze oxygenation of naturally occurring poly-unsaturated fatty acids (PUFAs) such as arachidonic acid and linoleic acid [3]. More importantly, lipoxygenases are involved in the regulation of inflammatory responses that can promote human disease. For example, human 5-lipoxygenase (5-HLO), human 12- lipoxygenase (12-HLO) and human 15- lipoxygenase (15-HLO) are involved in several diseases like asthma, arthritis, allergy, psoriasis, atherosclerosis and tumorigenesis [4-9].

The mechanism of lipoxygenase inhibition by inhibitors are classified into two groups, redox and nonredox inhibition. The redox active compound reduces lipoxygenase from ferric oxidation state to its inactive ferrous form where as allosteric inhibition can occur in nonredox mechanism [10, 11]. Puupehenone, a biologically active terpenoid, is a redox inhibitor of lipoxygenases most likely due to its relationship with the o-quinone (puupehedienone) shown in Figure 5.1 [12].

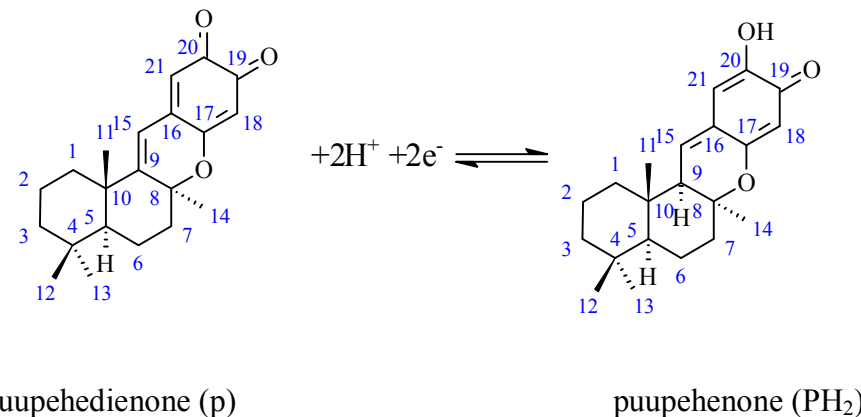
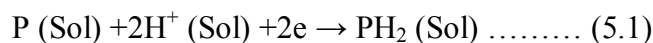


Figure 5.1. The two protons, two electron redox process of ppupehenone

In this study, we have calculated the redox potential of ppupehenone (PH₂) and its oxidized form i.e. ppupehediene (P) by using DFT method. In aqueous medium, ppupehediene and ppupehenone are capable of forming hydrogen bonds with water. Hence the influence of hydrogen-bond on the redox reaction was also investigated.

5.2. Computational details

All quantum chemical calculations were performed using Firefly [13]. To get the redox potential, it is required to calculate the standard free energy change (ΔG^0) for reaction (5.1).



The relation between ΔG^0 and absolute reduction potential is given by

$$E^0 = -\Delta G^0/nF \dots\dots\dots (5.2)$$

Where n is the number moles of electrons transferred in the reaction, which is equal to 2 for reaction (5.1), and F is the Faraday (96485 coulomb/mole).

To get ΔG^0 from computation, the following thermodynamic cycle (Figure 5.2) is used. This thermodynamic cycle involved all the species in the reaction (5.1) from gas to solution phase. Using this thermodynamic cycle, ΔG^0 (total) can be written as

$$\Delta G^0 \text{ (total)} = \Delta G^0 \text{ (g)} + \Delta G^0 \text{ (solv, PH}_2\text{)} - \Delta G^0 \text{ (solv, P)} - 2\Delta G^0 \text{ (solv, H}^+\text{)} \dots\dots\dots (5.3)$$

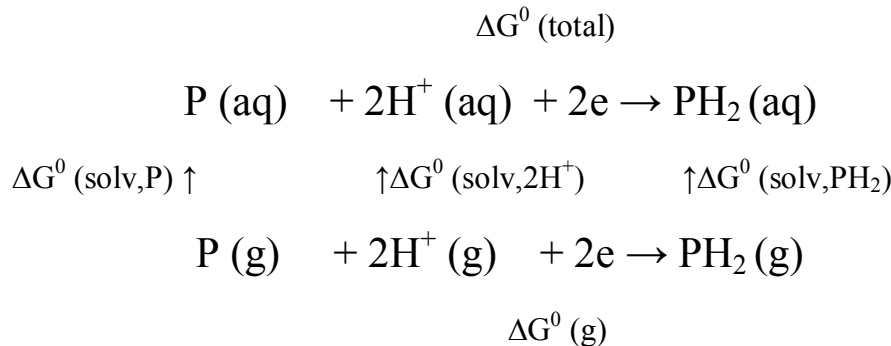


Figure 5.2. Thermodynamic cycle for obtaining ΔG^0 (total)

Where $\Delta G^0 \text{ (g)}$ is the Gibbs free energy of reaction (5.1) in gas phase. $\Delta G^0 \text{ (solv, PH}_2\text{)}$, $\Delta G^0 \text{ (solv, P)}$ and $\Delta G^0 \text{ (solv, H}^+\text{)}$ are the solvation Gibbs free energy of PH_2 , P and H^+ respectively. The standard Gibbs free energy of each molecule in the standard state at gas phase is obtained by equation (5.4) [14].

$$\Delta G^0_{(g)} = E_{0k} + ZPE + \Delta \Delta G_{0 \rightarrow 298} \dots\dots\dots (5.4)$$

Where E_{0k} and ZPE are the energy at 0K and zero point energy respectively. $\Delta \Delta G_{0 \rightarrow 298}$ is the Gibbs free energy change from 0 to 298K at 1 atm. An extra term $RT \ln(24.46)$ should be added in equation (5.4) to convert $\Delta G^0_{(g)}$ state from 1 atm to 1 M.

$$\Delta G^0_{(g)} (1M) = \Delta G^0_{(g)} (1 \text{ atm}) + RT \ln(24.46) = \Delta G^{0 \rightarrow *}\dots\dots\dots (5.5)$$

The $\Delta G^0_{(\text{solv})}$ can be calculated as the subtraction of the standard free energy of aqueous phase, $\Delta G^0_{(\text{aq})}$ and gas phase, $\Delta G^0_{(\text{g})}$.

$$\Delta G^0_{(\text{solv})} = \Delta G^0_{(\text{aq})} - \Delta G^0_{(\text{g})} \dots\dots\dots (5.6)$$

To calculate $\Delta G^0_{(\text{g})}$, we optimized the molecular structure of P and PH_2 at the DFT- B3LYP/6-311G(d,p) level of theory separately (Figure 5.3). Frequency calculations were performed at the same level of theory and basis set to verify that structure lies in the global minima and obtains the free energy of P and PH_2 . The standard free energy of electron is obtained by using its energy ($3.720\text{ kJ}\cdot\text{mol}^{-1}$) and entropy ($0.022734 \text{ kJ mol}^{-1}\text{K}^{-1}$) at 298 K[15]. The reported value of Gibbs free energy of H^+ (g) to be $-26.3 \text{ kJ}\cdot\text{mol}^{-1}$ [16].

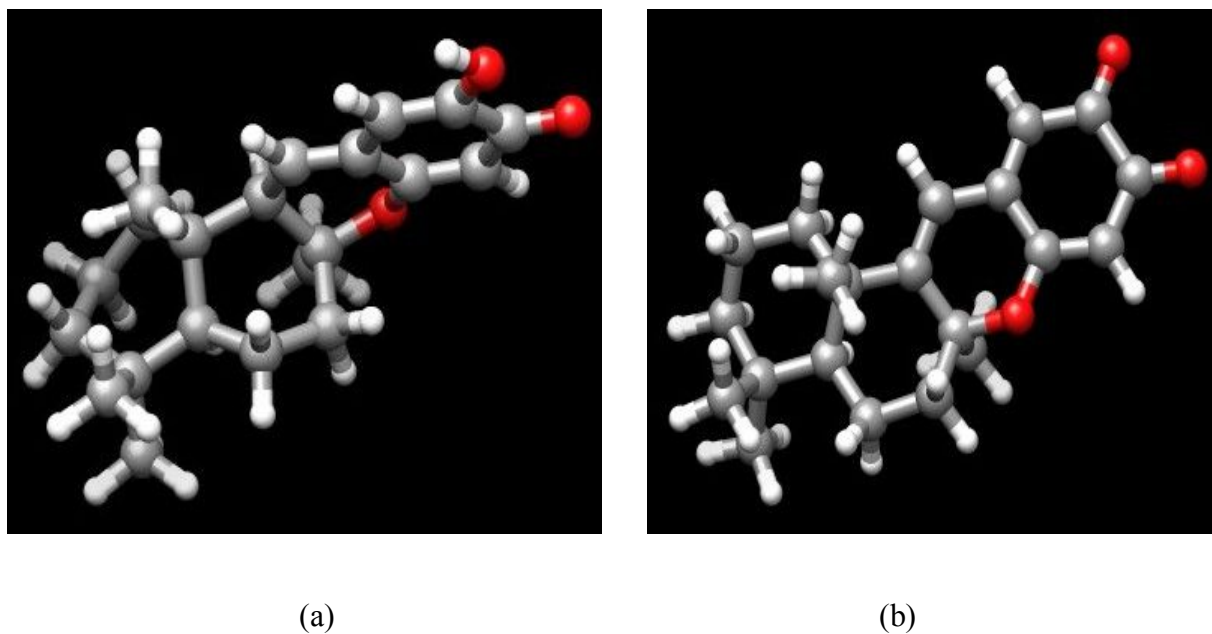


Figure 5.3. Optimized geometries of PH_2 (a) and P (b) at B3LYP/6-311G(d,p) level in gas phase

In order to compute $\Delta G^0_{(\text{aq})}$, the molecular structure of P and PH_2 were re-optimized by PCM model using water as a solvent at the same level of theory and basis set (Figure 5.4). Vibrational frequency calculations were performed to the optimized structures to get free energy of P and PH_2 . We have used the literature value of $-1104.6 \text{ kJ}\cdot\text{mol}^{-1}$ for $\Delta G^0_{(\text{solv}, \text{H}^+)} [17]$. It should be mentioned that this value is the change in the standard Gibbs free energy of reaction (5.1) in

solution in the standard state of gas phase (1 atm)[18]. To obtain the standard free energy of relation (5.3) in solution (1 mol/L) from gas phase (1 atm), it is necessary to add $\Delta n\Delta G^{0 \rightarrow *}$ to ΔG^0 (total). In reaction (5.1) Δn is equal to -2 and $\Delta G^{0 \rightarrow *}$ is 7.9 kJ.mol⁻¹.

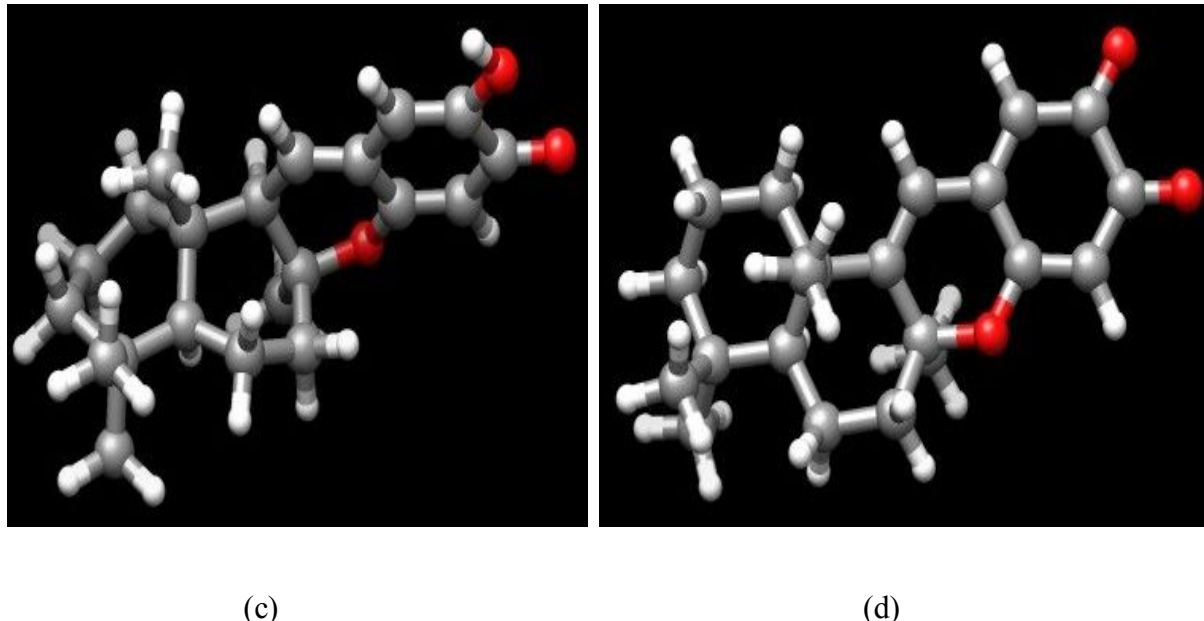


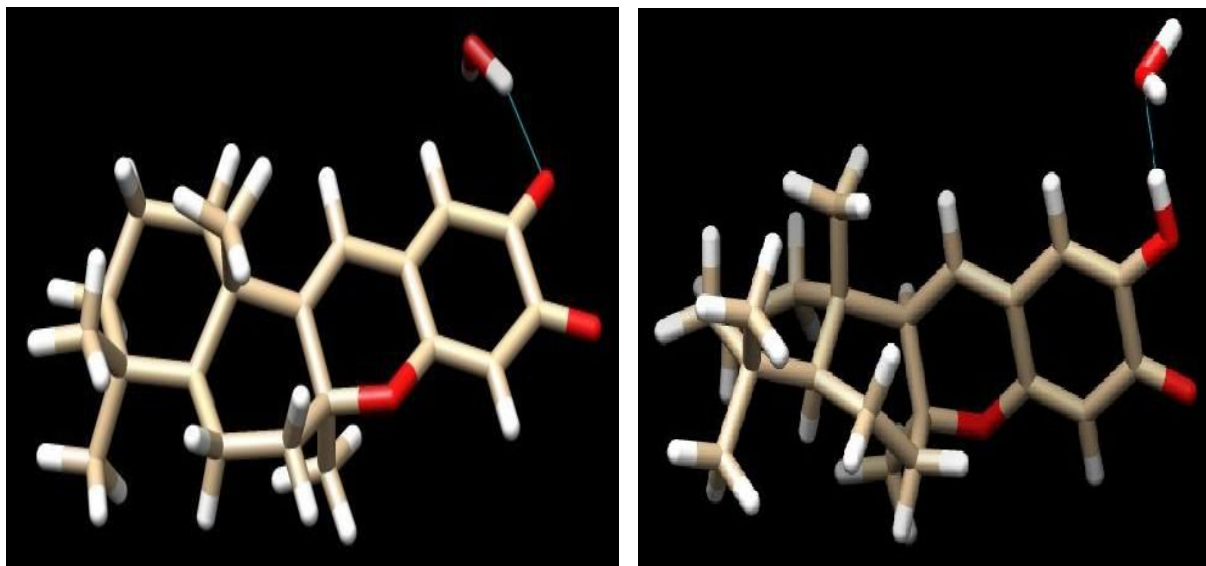
Figure 5.4. Optimized geometries of PH₂ (c) and P (d) at B3LYP/6-311G(d,p) level in water

To investigate the effect of H-bonding interactions on the redox potential of P/PH₂ system, we have microsolvated both ppupehedieneone (P) and ppupehenone (PH₂) on the carbonyl or hydroxyl group at C-20 with one to three water molecule(s). The hydrated complexes were optimized at the B3LYP/6-31G(d) level of theory in gas phase and performed the frequency calculations for the optimized low energy structures to determine the true local minima. The interaction energy (ΔE), which is defined as $\Delta E = E_M \dots n(w) - E_M - nE_w$, is calculated with each hydrated complex . Also, to predict the extra stability of the hydrated PH₂ complex than P complex, the difference in the interaction energy (ΔE_{diff}) and the difference in the solvation free energy (ΔG_{diff}) are calculated. ΔE_{diff} and ΔG_{diff} are given by:

$$\Delta E_{\text{diff}} = \Delta E(\text{PH}_2 \text{ complex}) - \Delta E(\text{P complex}) \dots\dots\dots (5.7)$$

$$\Delta G_{\text{diff}} = \Delta G(\text{solv}, \text{PH}_2 \text{ complex}) - \Delta G(\text{solv}, \text{P complex}) \dots\dots\dots (5.8)$$

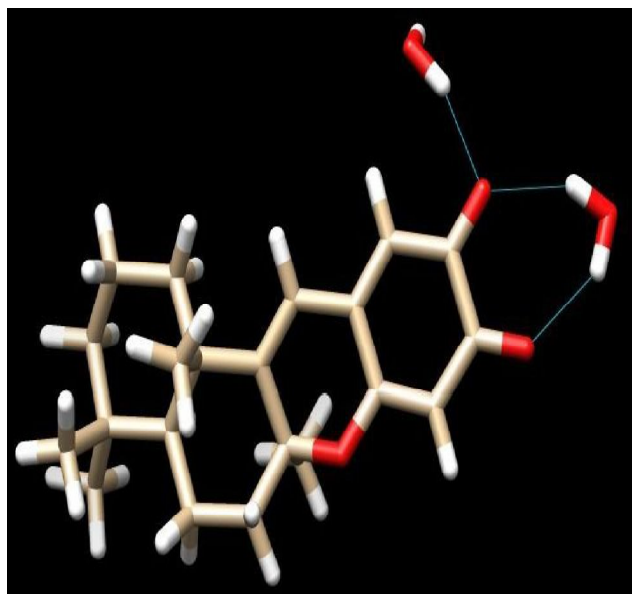
Optimized geometries of complexes along with the interaction energy (ΔE) are given in Figure 5.5 to 5.7. The molecular plots were produced using the UCSF Chimera 1.9.



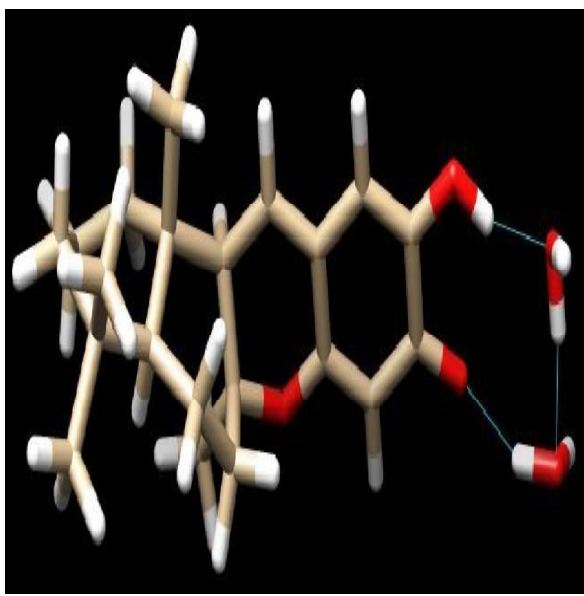
P-(H₂O)₁:ΔE=-39.04

PH₂-(H₂O)₁:ΔE=-43.00

Figure 5.5. Optimized geometries of puupehedieneone (P) and puupehenone (PH₂) with one water molecule along with ΔE (kJmol⁻¹)



P-(H₂O)_{2a} :ΔE=-74.22



PH₂-(H₂O)_{2a}:ΔE=-140.64

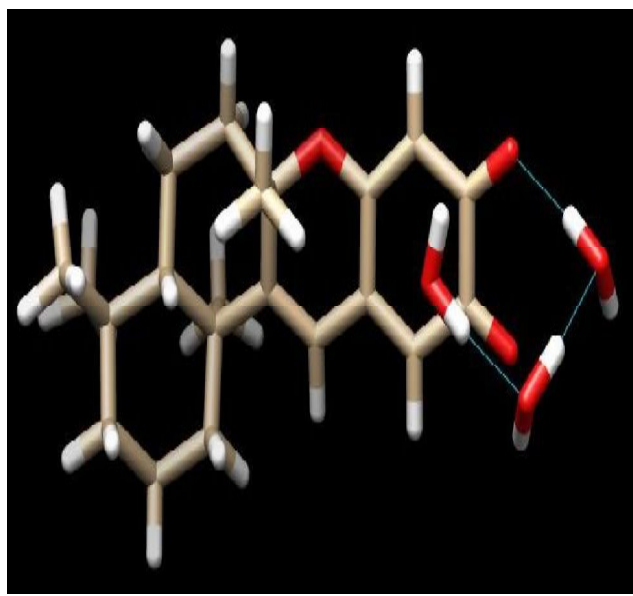


P-(H₂O)_{2b} :ΔE=-92.81

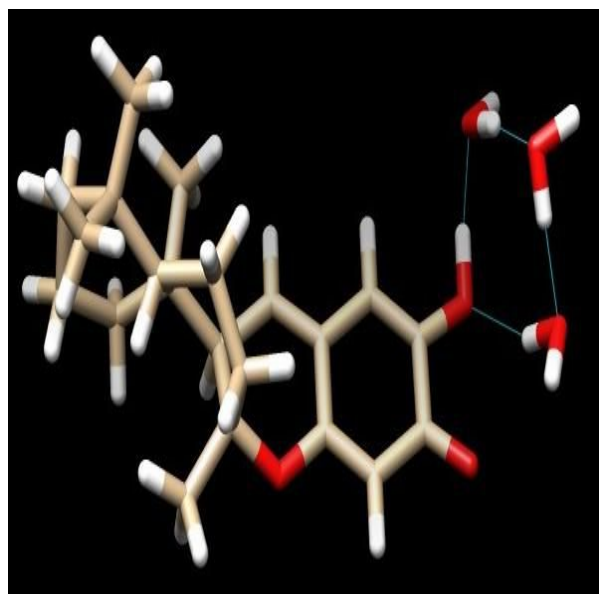


PH₂-(H₂O)_{2b}.ΔE=-94.89

Figure 5.6. Optimized geometries of puupehediene (P) and puupehenone (PH₂) with two water molecules at different configurations along with ΔE (kJmol⁻¹)



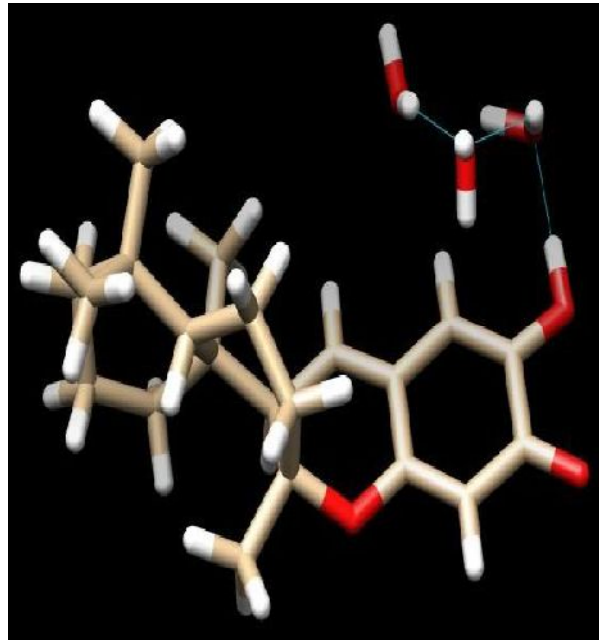
P-(H₂O)_{3a}:ΔE=-157.57



PH₂-(H₂O)_{3a}:ΔE=-190.72



P-(H₂O)_{3b}:ΔE=-152.19



PH₂-(H₂O)_{3b}:ΔE=-146.12

Figure 5.7. Optimized geometries of puupehedienone (P) and puupehenone (PH₂) with three water molecules at different configurations along with ΔE (kJmol⁻¹)

5.3. Results and discussion

In redox reaction, the thermodynamic cycle linking the process in the gas phase with that in solvent can be used to evaluate the reaction free energy. The free energy of the studied molecules and the redox potential are tabulated in Table 5.1. The standard free energy change of reaction (5.1) in solution, ΔG^0 (total) is equal to -785.481907 kJ.mol⁻¹ (at 6-311G** level). Using the value of ΔG^0 (total) and relation (5.2), the absolute reduction potential of P/PH₂ has been calculated in the order 4.07V. The absolute redox potential of SHE is 4.44V, so the E⁰ value of P/PH₂ system is in the order -0.370V.

Table 5.1. The Gibbs free energy of P and PH₂ in gas phase and solution, together with solvation free energies of species calculated at 6-31G* and 6-311G** basis set.

Basis set used	6-31G*		6-311G**	
Compounds	P	PH ₂	P	PH ₂
B3LYP Free Energy (g)/ (a.u)	-1040.711281	-1041.855358	-1040.994739	-1042.147231
B3LYP Free Energy (aq)/ (a.u)	-1040.729337	-1041.877011	-1041.015038	-1042.171998
ΔG^0 (solv)/kJmol ⁻¹	-47.406023	-56.849946	-53.295019	-65.025752
ΔG^0 (g)/kJmol ⁻¹	-2945.057593		-2967.151174	
ΔG^0 (total)/kJmol ⁻¹	-761.101516		-785.481907	
Absolute redox potential	3.944		4.070	
E ⁰ /V	-0.496		-0.370	

The reduction potential of the ferric ion in soybean lipoxygenase-1 versus normal hydrogen electrode has been estimated to be in excess of 0.5 V [19]. Hence the inhibitors in this class must

be weak reducing agents to reduce the ferric ion to the inactive ferrous state and ppupehenone may serve this purpose well.

The next objective of our study is to investigate the effect of hydrogen bonds on redox potentials. Figure 5.5 depicts the optimized geometry of ppupehedienone (P) and ppupehenone (PH_2) with one water molecule at B3LYP/6-31G* level of theory. Both ppupehedienone (P) and ppupehenone (PH_2) form one hydrogen bond with interaction energies are $-39.04 \text{ kJmol}^{-1}$ and -43 kJmol^{-1} respectively. Hence the difference in the interaction energy (ΔE_{diff}) is -3.96 kJmol^{-1} . Figure 5.6 depicts the optimized geometry of ppupehedienone (P) and ppupehenone (PH_2) with two water molecules at different configurations and it was found that the difference in the interaction energy is greater in $\text{P-(H}_2\text{O)}_{2a}/\text{PH}_2\text{-(H}_2\text{O)}_{2a}$ than $\text{P-(H}_2\text{O)}_{2b}/\text{PH}_2\text{-(H}_2\text{O)}_{2b}$. Figure 5.7 depicts the optimized geometry of ppupehedienone (P) and ppupehenone (PH_2) with three water molecules at different configurations. The difference in the interaction energy of $\text{P-(H}_2\text{O)}_{3a}/\text{PH}_2\text{-(H}_2\text{O)}_{3a}$ and $\text{P-(H}_2\text{O)}_{3b}/\text{PH}_2\text{-(H}_2\text{O)}_{3b}$ complexes are $-33.15 \text{ kJmol}^{-1}$ and 6.07 kJmol^{-1} respectively. Difference in the interaction energies (ΔE_{diff}), difference in solvation free energy (ΔG_{diff}), ΔG^0 (total) and absolute E^0 are displayed in Table 5.2. The trends (cf. Table 5.2) suggest that ΔG^0 (total) or absolute E^0 of P/ PH_2 couple is highly dependent on ΔE_{diff} and ΔG_{diff} .

Table 5.2. Difference in the interaction energies (ΔE_{diff}), difference in solvation free energy (ΔG_{diff}), ΔG^0 (total) and absolute E^0 of ppupehedienone (P) and ppupehenone (PH₂) complexes with different water molecules

Couple	ΔE_{diff} kJmol ⁻¹	ΔG_{diff} kJmol ⁻¹	ΔG^0 (total) kJmol ⁻¹	Absolute E^0 /V
P/PH ₂ -(H ₂ O) ₁	-3.96	-4.94	-756.598784	3.921
P/PH ₂ -(H ₂ O) _{2a}	-66.42	-54.59	-806.247371	4.178
P/PH ₂ -(H ₂ O) _{2b}	-2.08	-5.47	-757.126509	3.924
P/PH ₂ -(H ₂ O) _{3a}	-33.15	-31.24	-782.895789	4.057
P/PH ₂ -(H ₂ O) _{3b}	6.07	-5.73	-445.923501	3.865
P/PH ₂ -(PCM)	-4.25	-9.44	-761.101516	3.944

5.4. Conclusion

The standard reduction potential of Fe⁺³/ Fe⁺² couple is 0.77V and it is expected that the reduction potentials of lipoxygenases are lower than this value. However the exact reduction potential of the ferric ion in 5-HLO, 12-HLO and 15-HLO are not known. Hence this study helps to predict the E^0 value of different lipoxygenases. Since ppupehedienone and ppupehenone are capable of forming hydrogen bond with water, the absolute value of E^0 of P/PH₂ couple is highly dependent on ΔE_{diff} and ΔG_{diff} .

5.5 References

- [1] E.I. Solomon, J. Zhou, F. Neese, E.G. Pavel, New insights from spectroscopy into the structure/function relationships of lipoxygenases, Chem Biol. 4 (1997) 795-808.

- [2] H.W. Gardner, Biological roles and biochemistry of the lipoxygenase pathway, HortScience. 30 (1995) 197-205.
- [3] R. Wisastra, F.J. Dekker, Inflammation, cancer and oxidative lipoxygenase activity are intimately linked, Cancers. 6 (2014) 1500-1521.
- [4] L.A. Dailey, P. Imming, 12-Lipoxygenase: classification, possible therapeutic benefits from inhibition, and inhibitors, Curr Med Chem. 6 (1999) 389-398.
- [5] V.E. Steele, C.A. Holmes, E.T. Hawk, L. Kopelovich, R.A. Lubet, J.A. Crowell, C.C. Sigman, G.J. Kelloff, Lipoxygenase inhibitors as potential cancer chemopreventives, Cancer Epidemiol Biomarkers Prev. 8 (1999) 467-483.
- [6] B. Samuelsson, S.E. Dahlen, J.A. Lindgren, C.A. Rouzer, C.N. Serhan, Leukotrienes and lipoxins: structures, biosynthesis, and biological effects, Science. 237 (1987) 1171-1176.
- [7] X.Z. Ding, W.G. Tong, T.E. Adrian, 12-Lipoxygenase metabolite 12(S)-HETE stimulates human pancreatic cancer cell proliferation via protein tyrosine phosphorylation and ERK activation, Int J Cancer. 94 (2001) 630-636.
- [8] J.A. Cornicelli, B.K. Trivedi, 15-Lipoxygenase and its inhibition: a novel therapeutic target for vascular disease, Curr Pharm Des. 5 (1999) 11-20.
- [9] U.P. Kelavkar, J.B. Nixon, C. Cohen, D. Dillehay, T.E. Eling, K.F. Badr, Overexpression of 15-lipoxygenase-1 in PC-3 human prostate cancer cells increases tumorigenesis, Carcinogenesis. 22 (2001) 1765-1773.
- [10] C. Kemal, P. Louis-Flamberg, R. Krupinski-Olsen, A.L. Shorter, Reductive inactivation of soybean lipoxygenase-1 by catechols: a possible mechanism for regulation of lipoxygenase activity, Biochemistry. 26 (1987) 7064-7072.

- [11] R. Mogul, E. Johansen, T.R. Holman, Oleyl sulfate reveals allosteric inhibition of soybean lipoxygenase-1 and human 15-lipoxygenase, *Biochemistry*. 39 (2000) 4801-4807.
- [12] T. Amagata, S. Whitman, T.A. Johnson, C.C. Stessman, C.P. Loo, E.L. Jonclardy, P. Crews, T.R. Holman, Exploring sponge-derived terpenoids for their potency and selectivity against 12-human, 15-human, and 15-soybean lipoxygenases, *J Nat Prod.* 66 (2003) 230-235
- [13] A.A. Granovsky, Firefly version 8, [www](http://classic.chem.msu.su/gran/firefly/index.html)
<http://classic.chem.msu.su/gran/firefly/index.html>.
- [14] Y.H. Jang, W.A. Goddard III, K.T. Noyes, L.C. Sowers, S. Hwang, D.S. Chung, pKa Values of guanine in water: density functional theory calculations combined with poisson-boltzmann continuum-solvation model, *J Phys Chem B.* 107 (2003) 344-357.
- [15] J.E. Bartmess, Thermodynamics of the electron and the proton, *J Phys Chem.* 98 (1994) 6420-6424.
- [16] M.D. Liptak, K.G. Gross, P.G. Seybold, S. Feldgus, G.C. Shields, Absolute pK(a) determinations for substituted phenols, *J Am Chem Soc.* 124 (2002) 6421-6427.
- [17] P. Winget, E.J. Weber, C.J. Cramer, D.G. Truhlar, Computational electrochemistry: aqueous one-electron oxidation potentials for substituted anilines, *Phys Chem Chem Phys.* 2 (2000) 1231-1239.
- [18] N.S. Babu, Computational studies for oxidation reduction reactions of cinnoline - 4(1H)-one, in aqueous phase by density functional theory, *BJAST.* 4 (2014) 465-476.
- [19] M.J. Nelson, D.G. Batt, J.S. Thompson, S.W. Wright, Reduction of the active-site iron by potent inhibitors of lipoxygenases, *J Biol Chem.* 266 (1991) 8225-8229.